Mol. Cells *33*, 79-86, January 31, 2012
DOI/10.1007/s10059-012-2228-y

Molecules and Cells

In Vivo Imaging of Differences in Early Donor Cell Proliferation in Graft-Versus-Host Disease Hosts with Different Pre-Conditioning Doses

Myung Geun Song[1,2,3,9], Bora Kang[4,9], Ji Yeong Jeon[4], Jun Chang[5], Seungbok Lee[6], Chang-Ki Min[7], Hyewon Youn[2,3,8,*], and Eun Young Choi[4,*]

Graft-versus-host disease (GVHD) results from immune-mediated attacks on recipient tissues by donor-originated cells through the recognition of incompatible antigens expressed on host cells. The pre-conditioning irradiation dose is a risk factor influencing GVHD severity. In this study, using newly generated luciferase transgenic mice on a B6 background (B6.Luc^{Tg}) as bone marrow and splenocyte donors, we explored the effects of irradiation doses on donor cell dynamics in major histocompatibility complex (MHC)-matched allogeneic GVHD hosts via bioluminescence imaging (BLI). Results from BLI of GVHD hosts showed higher emission intensities of luminescence signals from hosts irradiated with 900 cGy as compared with those irradiated with 400 cGy. In particular, BLI signals from target organs, such as the spleen, liver, and lung, and several different lymph nodes fluctuated with similar time kinetics soon after transplantation, reflecting the synchronous proliferation of donor cells in the different organs in hosts irradiated with 900 cGy. The kinetic curves of the BLI signals were not synchronized between the target organs and the secondary organs in hosts irradiated with 400 cGy. These results demonstrate that pre-conditioning doses influence the kinetics and degree of proliferation in the target organs soon after transplantation. The results from this study are the first describing donor cell dynamics in MHC-matched allogeneic GVHD hosts and the influence of irradiation doses on proliferation dynamics, and will provide spatiotemporal information to help understand GVHD pathophysiology.

INTRODUCTION

Graft-versus-host disease (GVHD) is an obstacle for the application of allogeneic hematopoietic stem-cell transplantation (HSCT) in curative therapies of hematological malignancies and immunologic diseases. The disease results from immune-mediated attacks on recipient tissues by donor-originated T cells, which recognize disparities between donors and recipients at multiple genetic loci (Shlomchik, 2007). Mismatches at major histocompatibility complex (MHC) loci between stem cell donors and recipients is a major risk factor for GVHD development (Ferrara et al., 1999; Yoon et al., 2007). In MHC-matched bone marrow (BM) transplantation, disparities at minor histocompatibility (H) antigen loci drive the allo-responses of donor T cells and contribute to the development of GVHD (Choi et al., 2001; 2002a; 2002b; Korngold and Wettstein, 1990; Roopenian et al., 2002).

The intensity of pre-conditioning of recipients prior to HSCT (for example, total body irradiation) is another risk factor influencing GVHD severity (Ferrara et al., 2009). Pre-conditioning allows ablation of the recipient's bone marrow and enhances engraftment of donor hematopoietic stem cells; however, it also provokes damage to the epithelial lining and the release of inflammatory cytokines, such as interleukin-1 (IL-1), IL-6, tumor necrosis factor α (TNF-α), and interferon γ (IFN-γ). This early release of cytokines activates antigen presenting cells (APCs), resulting in the activation and proliferation of allo-reactive T cells (Ferrara et al., 2009).

Bioluminescence imaging (BLI) is a sensitive tool that enables noninvasive *in vivo* monitoring of cells and provides important information on the biodistribution, proliferation, and persistence of cells (Cao et al., 2005; Panoskaltsis-Mortari et al., 2004; Weissleder and Pittet, 2008). For this reason, this technique has been used to track immune cells during GVHD, usually under MHC-mismatched conditions. After transplantation of luciferase-expressing bone marrow (BM) and leukocytes from FVB^{luc+} mice into irradiated BALB/c mice, which are a MHC-

[1]Department of Tumor Biology, Seoul National University College of Medicine, Seoul 110-799, Korea, [2]Department of Nuclear Medicine, Seoul National University College of Medicine, Seoul 110-799, Korea, [3]Laboratory of Molecular Imaging and Therapy, Cancer Research Institute, Seoul National University College of Medicine, Seoul 110-799, Korea, [4]Department of Biomedical Sciences, Seoul National University College of Medicine, Seoul 110-799, Korea, [5]Division of Life and Pharmaceutical Sciences, Ewha Womans University, Seoul 120-750, Korea, [6]Department of Cell and Developmental Biology, School of Dentistry, Seoul National University, Seoul 110-749, Korea, [7]Department of Internal Medicine, The Catholic University of Korea College of Medicine, St. Mary's Hospital, Seoul 137-701, Korea, [8]Cancer Imaging Center, Seoul National University Cancer Hospital, Seoul 110-799, Korea, [9]These authors contributed equally to this work.
*Correspondences: eycii@snu.ac.kr (EYC); hwyoun@snu.ac.kr (HY)

Received October 7, 2011; revised October 18, 2011; accepted October 19, 2011; published online January 3, 2012

Keywords: bioluminescence imaging, graft-versus-host disease, irradiation dose, luciferase, transgenic mouse

mismatched recipient strain (FVB → BALB/c), cells were detected in the secondary lymphoid organs within 1 day after transplantation and spread into the intestine, liver, and skin during GVHD development (Beilhack et al., 2005; Zhang et al., 2002).

Previously, we demonstrated the induction of acute GVHD by transplantation of BM and splenocytes from C57BL/6 (B6) mice into irradiated BALB.B mice (B6 → BALB.B), a mouse strain matched at the MHC locus, but disparate at other loci compared with the B6 strain (Choi et al., 2002a; 2011). During the B6 → BALB.B GVHD, minor H-antigen-specific CD8 T cells were detected in the blood and target organs, such as the spleen, lung, and liver, of the BALB.B hosts. Pre-conditioning of the host with 900 cGy-irradiation resulted in very low survival of the BALB.B hosts (100% mortality rate by day 42 post-transplantation) with serious weight loss, while hosts irradiated with 400 cGy survived longer than 56 days with mild weight changes (Choi et al., 2011). This difference in GVHD severity, depending on irradiation dose, was accompanied by different kinetics and compositions of leukocytes infiltrating GVHD target organs (liver, lung, and spleen) according to a fluorescence-activated cell sorting (FACs) profiling study (Choi et al., 2011). However, where, how, and when such differences induced by different pre-conditioning doses develop is not yet clearly understood. In addition, the lack of luciferase-expressing transgenic mice on a genetically controlled B6 background hampered the investigation of donor cell dynamics in MHC-matched allogeneic GVHD hosts. Moreover, the fact that allo-responses under the MHC-matched condition are weaker than under the MHC-mismatched condition requires donor mouse strains that efficiently express the reporter protein in order to detect the less vigorous donor cell proliferation in the MHC-matched allogeneic GVHD hosts.

In this study, we report the generation of a transgenic mouse line on a B6 background that expresses luciferase with efficient enzyme activity (B6.Luc^{Tg}). In addition, we describe the results of BLI of BALB.B GVHD hosts with different pre-conditioning doses using B6.Luc^{Tg} mice as BM and splenocyte donors.

MATERIALS AND METHODS

Mice

C57BL/6 (B6: H-2^b) and C.B10-*H2^b*/LiMcdj (BALB.B: H-2^b) mice were purchased from the Jackson laboratory (USA). Luciferase transgenic mouse lines were generated after microinjection of a DNA fragment, including promoter, luciferase coding, and poly A signal sequences, into fertilized eggs from B6 mice (B6.Luc^{Tg}). This strain was maintained by crossing with B6 mice at the Center for Animal Resource Development, Seoul National University College of Medicine. The transgenic mice ubiquitously express a codon-optimized firefly luciferase (Rabinovich et al., 2008) and one founder line out of 11 different founders was selected for its high level of luciferase activity. The induction of GVHD and subsequent bioluminescence imaging was performed under approval from the Seoul National University Institutional Animal Care and Use Committee (IACUC).

Induction of allo-responses and GVHD

To induce an allo-response, female B6 or B6.Luc^{Tg} mice were intraperitoneally (i.p.) injected with splenocytes (2×10^7) from BALB.B mice. Mice were periodically bled for flow cytometric analysis of the antigenic-specificity of peripheral blood lymphocytes (PBL). For induction of GVHD, bone marrow cells (BM) and splenocytes were prepared from wild-type or B6.Luc^{Tg} mice. Mixtures of BM (5×10^6) and splenocytes (2×10^7) in 1× phosphate buffered saline (PBS) were intravenously injected into irradiated BALB.B mice. Recipient BALB.B mice were pre-conditioned with two split doses of either 900 cGy or 400 cGy from a ^{137}Cs source with a 5 h interval. Mice were then transplanted with the BM/splenocyte mixture 5 h after the second irradiation.

In vivo imaging

In vivo bioluminescence imaging was performed using an IVIS 100 imaging system with a charge-coupled device (CCD) camera (Caliper Life Sciences, USA). Mice were kept on the imaging stage under anesthesia with 1.5% isoflurane gas in oxygen at a flow rate of 1.5 L/min and were given an i.p. injection of the substrate, D-luciferin (150 mg/kg body weight; Molecular Probes, USA). Mice were positioned supine to image the ventral surface or on the left side to reveal the spleen. *In vivo* BLI was collected at 10-15 min (0 h), 5, 12, and 24 h, and 2, 4, 8, 14, and 21 days after GVHD induction.

Analysis of bioluminescence data

Relative intensities of emitted light were presented as pseudocolor images raging from red (most intense) to blue (least intense). Gray-scale photographs and the corresponding pseudocolor images were superimposed with LIVINGIMAGE (ver 2.12; Xenogen) and IGOR (WaveMetrics, USA) image analysis software. Signals emitted by regions of interest (ROI) were measured and data were expressed as photon flux [photon s^{-1} cm^{-2} steradian^{-1} (sr^{-1})], which refers to the photons emitted from a unit solid angle of a sphere. Data are presented as the mean ± standard error of the mean (SEM). The machine background was subtracted electronically, both from the images and from the measurements of photon flux.

Ex vivo imaging and analysis

After *in vivo* BLI, mice were injected with an additional dose of D-luciferin (150 mg/kg body weight). Five minutes later, the animals were sacrificed and the organs were prepared and imaged. Single cell suspensions were prepared from the spleen, thymus, and peripheral blood, and placed into 48-well tissue culture plates. CD3$^+$, B220$^+$, and CD3$^-$B220$^-$ cells were MACS purified from the spleen of wild-type B6 and B6.Luc^{Tg} mice according to the manufacturer's protocol (Miltenyi Biotec, USA) and placed into culture plates. Prior to imaging, 1 μl of D-luciferin (30 mg/ml) was added into each well containing cells.

Flow cytometry

Fresh PBLs from immunized B6 or B6.Luc^{Tg} mice were incubated at 4°C for 30 min in FACs buffer (1× PBS with 0.1% bovine calf serum and 0.05% sodium azide) containing PE-labeled H60/H-K^b tetramer and FITC-conjugated anti-CD11a (2D7, eBioscience, USA) and APC-conjugated anti-CD8 (eBioscience) monoclonal antibodies. Fresh PBLs, splenocytes, and thymocytes from B6 or B6.Luc^{Tg} mice were stained with PE or APC-conjugated anti-Mac-1 (M1/70, eBioscience), FITC-conjugated anti-Gr-1 (RB6-8C5, eBioscience), PE-conjugated anti-CD4 (GK1.5, eBioscience), and APC-conjugated anti-CD8 monoclonal antibodies. After staining, cells were re-suspended in FACs buffer and analyzed using a FACSCalibur equipped with CellQuest software (BD Bioscience, USA).

RESULTS

Generation of luciferase-expressing transgenic mice

We developed a universal donor transgenic mouse line that expresses luciferase in all tissues under the control of the

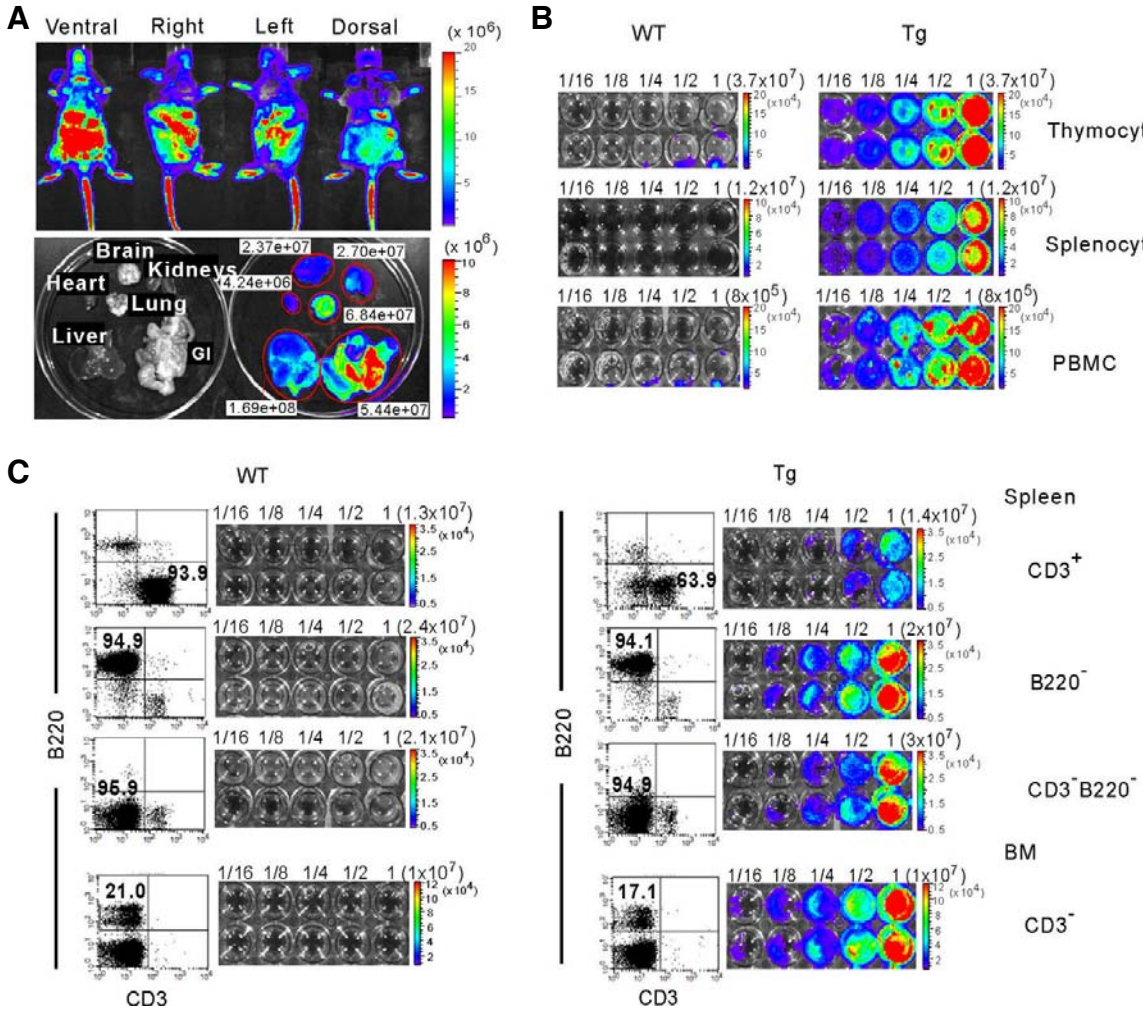

Fig. 1. Generation of luciferase-expressing transgenic mice. (A) Whole body bioluminescence imaging (BLI) and *ex-vivo* imaging demonstrate the expression of luciferase in all tissues of the transgenic mice. D-luciferin, a luciferase substrate, was given to the transgenic (Tg) and wild-type (WT) B6 mice 5 min before imaging. These data represent more than three independent experiments. (B) Single suspensions of thymocytes, splenocytes, and peripheral blood lymphocytes were prepared from the B6. Luc^{Tg} mice (Tg) and wild-type (WT) B6 mice. Cells were placed into 48-well plates as duplicates and serially diluted to determine the photon outcome per cell. D-luciferin was added to the medium solution in the wells. BLI was performed after 5 min. (C) T (CD3$^+$), B (B220$^+$), and non-T and B cells (CD3$^-$B220$^-$) were MACS purified using the splenocytes of Tg and WT B6 mice. They were distributed into 48-well plates and processed as described above for BLI. Single cell suspensions of bone marrow (BM) were prepared by flushing the tibia and femur of Tg and WT mice. After depletion of CD3$^+$ T cells, the BM cells were distributed into wells for BLI. The data shown are representative of two independent experiments.

chicken beta actin promoter using firefly luciferase with sequence modification by codon optimization to enhance the enzyme activity (eff-luciferase) (Rabinovich et al., 2008). We selected a transgenic line (#15), out of 11 different founder lines, which showed the highest luciferase activity detected in the peripheral blood leukocytes (data not shown). We maintained the line by successive crossing with B6 mice and named it B6.Luc^{Tg}.

In vivo luminescence imaging of the total body of B6.Luc^{Tg} mice confirmed the ubiquitous expression of the luciferase transgene (Fig. 1A). When photon flux emission from defined ROIs was measured after i.p. injection of the substrate, D-luciferin, the highest value was detected in the central abdominal region (2.1×10^9 s^{-1}cm^{-2}sr^{-1}), with other regions detected in a range of 1.4-5.8 $\times$ 10^8 s^{-1}cm^{-2}sr^{-1}. All of the organ explants from the B6.Luc^{Tg} mouse emitted signals in the range of 0.4-54 $\times$ 10^7 s^{-1}cm^{-2} sr^{-1}, with the highest intensity detected in the gastrointestinal tract.

Luciferase activity in hematopoietic cells of B6.Luc^{Tg} mice was determined using single cell suspensions of the thymus, spleen, and PBL. Thymocytes, splenocytes, and PBLs were prepared from B6.Luc^{Tg} mice and measured for the emission of bioluminescence signals by adding D-luciferin to the cell suspension medium and incubating for 1 min before detection. The signals detected were 0.13 s^{-1}cm^{-2}sr^{-1}, 0.29 s^{-1}cm^{-2}sr^{-1}, and 5.1 s^{-1}cm^{-2}sr^{-1} on average for thymocytes, splenocytes, and PBLs, respectively, while no signals were detected from wild-type B6 mice (Fig. 1B).

When luciferase activity was further measured for each leukocyte subtype (T, B, and non-T and B cells) in the B6.Luc^{Tg} mouse using the MACS-purified CD3$^+$, B220$^+$, and CD3$^-$B220$^-$ cells, respectively, the intensity of the bioluminescence signal

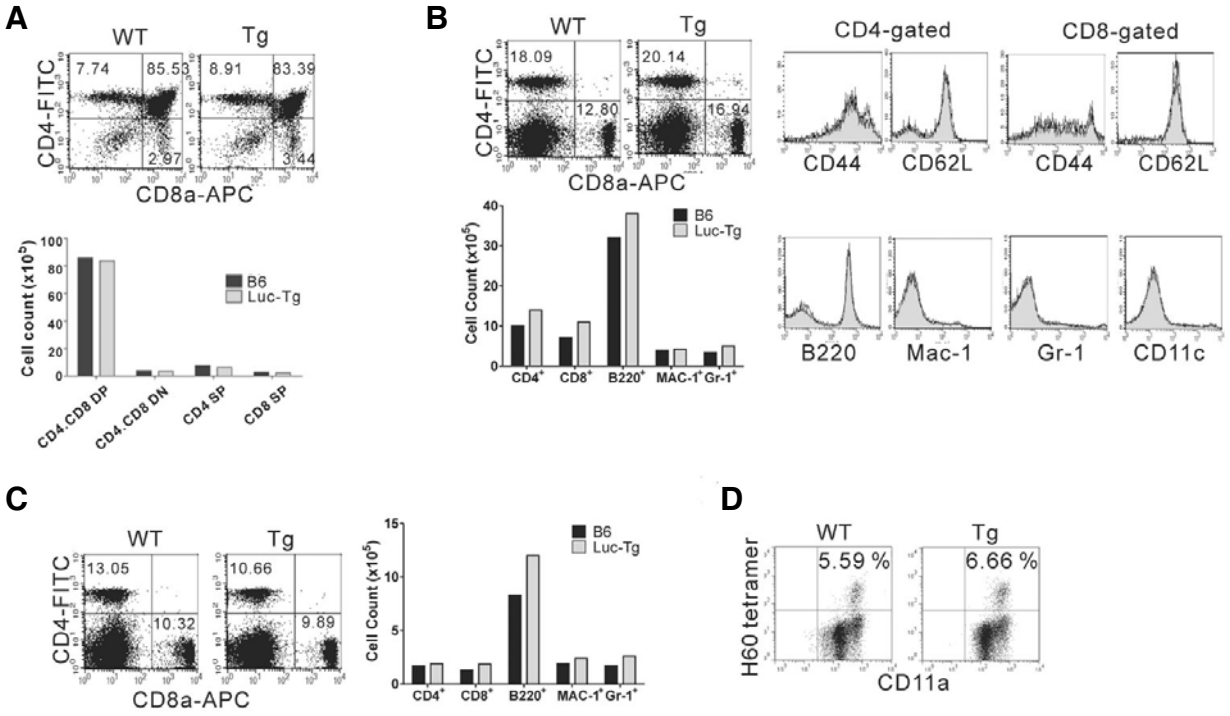

Fig. 2. Normal hematopoiesis and immunity in B6. Luc^{Tg} mice. (A) Thymocytes, (B) splenocytes, and (C) peripheral blood lymphocytes (PBL) from B6. Luc^{Tg} mice (Tg) and wild-type (WT) B6 mice were stained with monoclonal antibodies against marker proteins for cell population subtyping (CD4, CD8, B220, Mac-1, and Gr-1) and the activation proteins (CD44 and CD62L). Percentages of cells corresponding to the CD4$^-$ CD8$^-$ double negative, CD4$^+$CD8$^+$ double positive, CD4$^+$ single positive, or CD8$^+$ single positive cells in the thymus (A), and CD4$^+$ cells, CD8$^+$ cells, Mac-1$^+$ cells, or Gr-1$^+$ cells in the spleen (B) are shown. The numbers of each cell population were calculated by multiplying the total cell yield and the percentage values. To compare the levels of CD44 and CD62L expression in CD4 and CD8 T cells from the spleen (B) between Tg and WT B6 mice, overlays of single histograms for CD44 and CD62L are shown after gating on CD4$^+$ or CD8$^+$ cells. These data represent more than three independent experiments. (D) To investigate whether allo-responses could be induced normally in B6. Luc^{Tg} mice, female B6. Luc^{Tg} mice were injected intraperitoneally (i.p.) with splenocytes (2×10^7) from BALB.B mice, and PBLs collected from the three immunized mice were stained with PE-conjugated H60-H-2K^b tetramer, FITC-conjugated CD11a mAb, and APC-conjugated CD8 mAb. Flow cytometry analysis was performed using FACSCalibur equipped with CellQuest. H60-tetramer binding cells with CD11a^{high} phenotype are shown after gating on CD8$^+$ cells. WT B6 mice were immunized and analyzed with the same methods described above. The data represent two independent experiments.

was highest in the CD3$^-$B220$^-$ cells (1.7×10^{-1} s^{-1}cm^{-2}sr^{-1} on average), intermediate in the B cells (2.78×10^{-2} s^{-1}cm^{-2}sr^{-1}), and lowest in the T cells, (1.47×10^{-2} s^{-1}cm^{-2}sr^{-1}) (Fig. 1C). The average photon emission value for BM depleted of CD3$^+$ T cells was 2.2×10^{-1} photons s^{-1}cm^{-2}sr^{-1} (Fig. 1C). No cell subtypes from wild-type B6 mice emitted any luminescence signals. Results from BLI of leukocytes and each subtype confirmed the suitability of the B6.Luc^{Tg} mouse as a universal donor for leukocyte tracking.

Normal hematopoietic cell development and induction of allo-reactivity in B6.Luc^{Tg} mice

Prior to using cells from B6.Luc^{Tg} mice to track immune responses, we first examined whether hematopoiesis in the B6.Luc^{Tg} mouse was intact, without any influence from the transgene incorporation in the genome of the mice. Single cell suspensions of the thymus, spleen, and peripheral blood prepared from B6.Luc^{Tg} mice were analyzed via flow cytometry for comparison of cellular profiles with those obtained from wild-type B6 mice. The overall composition of the three organs was comparable between B6.Luc^{Tg} and wild-type B6 mice. The thymic profile of B6.Luc^{Tg} mice was normal, with percentages and numbers corresponding to CD4$^+$CD8$^+$ double positive, CD4$^+$ single positive, and CD8$^+$ single positive cells at appropriate ratios (80, 10, and 5%, respectively) (Fig. 2A). The composition of splenocytes and PBLs from B6.Luc^{Tg} mice was also within normal ranges according to flow cytometric analysis after staining with antibodies for cell markers [CD4, CD8, B220, CD11b (Mac-1$^+$), CD11c, and Gr-1] (Figs. 2B and 2C). Even the expression levels of CD44 and CD62L in CD4 and CD8 T cells from the spleen overlapped in B6.Luc^{Tg} and wild-type B6 mice. Based on these FACs profiling data, we confirmed that the development of hematopoietic lineage cells in B6.Luc^{Tg} mice is preserved.

We tested whether leukocytes from B6.Luc^{Tg} mice would be functional and able to generate immune responses against an antigenic challenge. For this, we induced an allo-response in B6.Luc^{Tg} mice by i.p. injection of splenocytes from BALB.B mice, which is a MHC-matched allogeneic strain, and analyzed the PBLs from immunized B6.Luc^{Tg} mice. Using flow cytometry we attempted to detect allo-antigen-specific CD8 T-cells in the blood after staining with peptide-MHC tetramers. Results from the flow cytometric analysis demonstrated that the frequencies of CD8 T cells specific for H60, a minor histocompatibility antigen, were in the range of 5 to 7% of CD8 T cells in the blood of the immunized mice at the peak of the immune response (day

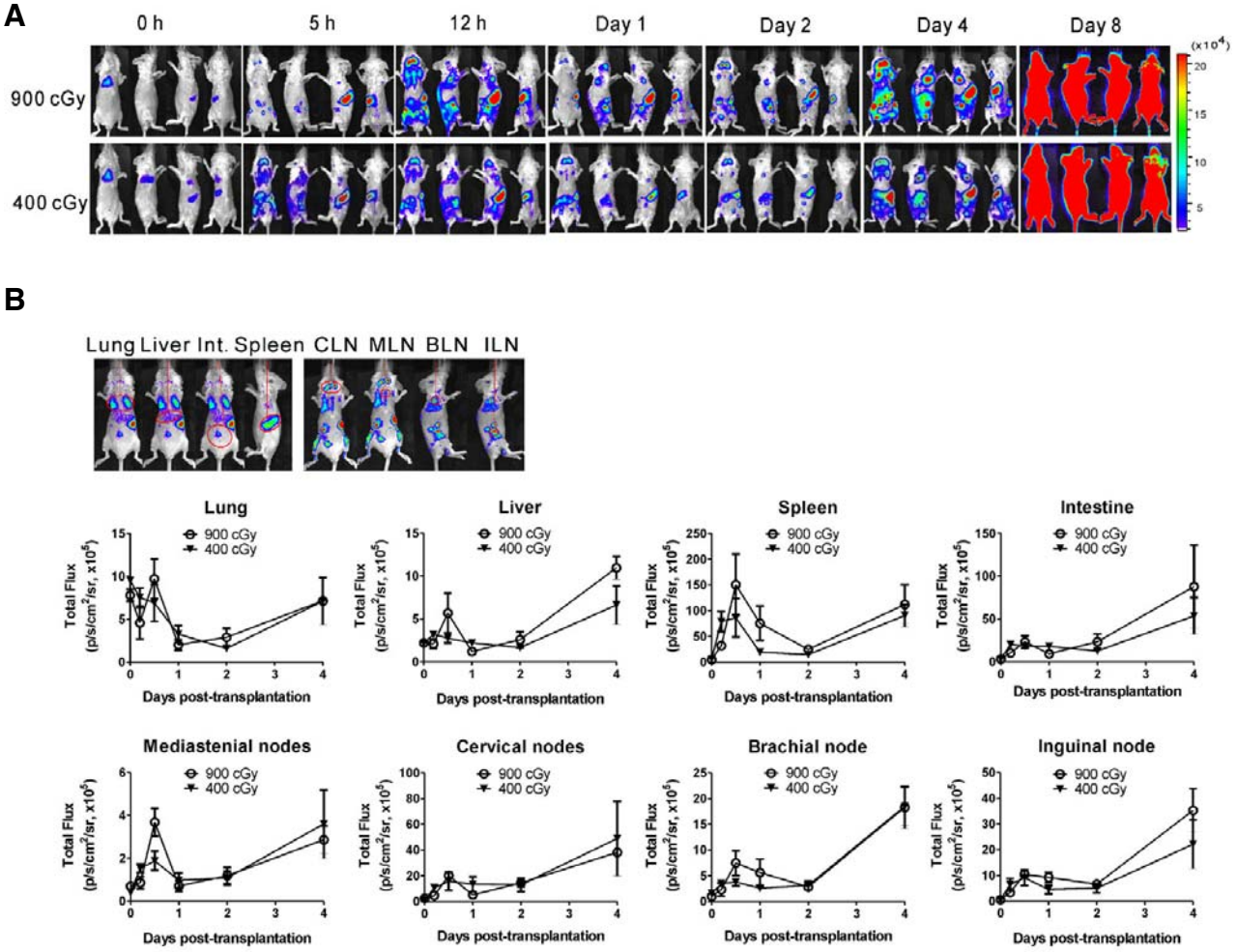

Fig. 3. Short-term kinetics of bioluminescence intensity after graft-versus-host disease (GVHD) induction in hosts pre-conditioned with different irradiation doses. (A) BALB.B GVHD hosts were transplanted with bone marrow (BM) cells (5×10^6) and splenocytes (2×10^7) from female B6.Luc^{Tg} mice after irradiation with 900 cGy or 400 cGy (n = 3 for each group). After transplantation, bioluminescence imaging (BLI) was performed regularly and the *in vivo* imaging results demonstrate proliferation and migration of donor cells in the hosts. One mouse from each group is shown. (B) To compare the donor cell distribution in the different irradiation groups along with GVHD development, regions of interest (ROIs) were defined for the spleen, liver, lung, and intestine (abdomen) as target organs, and for the mediastenial nodes (MLN), cervical nodes (CLN), brachial nodes (BLN), and inguinal nodes (ILN) as secondary lymphoid organs from three different mice. Total photon outcomes after 4 days from each ROI from three different mice are plotted along the time course for short-term events. Data are represented as mean ± standard error of the mean (SEM).

10 post-immunization) in both B6.Luc^{Tg} and wild-type B6 mice (Fig. 2D). Additionally, mixed leukocyte culture of splenocytes from the immunization of B6.Luc^{Tg} and B6 mice with irradiated BALB.B cells resulted in expansion of H60-specific CD8 T-cells *in vitro* (data not shown). All of these results verified that the leukocytes of B6.Luc^{Tg} mice could be used for tracking immune responses occurring in BALB.B hosts after GVHD induction. Immunization of B6.Luc^{Tg} and B6 mice with cells from either B6.Luc^{Tg} or B6 did not induce any immune response *in vivo* nor cell proliferation *in vitro*, demonstrating that the luciferase transgene is not immunogenic in B6 mice.

In vivo distribution of donor cells in GVHD hosts

Finally, we investigated donor cell dynamics in MHC-matched allogeneic GVHD hosts (BALB.B). In our previous study, we showed that BALB.B hosts irradiated with a 900 cGy dose had a very low survival rate with serious weight loss, while hosts irradiated with 400 cGy survived long with mild symptoms (Choi et al., 2011). Such differences in GVHD severity were thought to correlate with the degree of proliferation and tissue infiltration of the transplanted donor cells, depending on pre-conditioning doses.

To examine if there would be differences in the donor dynamics between hosts with different pre-conditioning doses, we used B6.Luc^{Tg} mice as BM and splenocyte donors to induce GVHD in BALB.B mice (B6.Luc^{Tg} → BALB.B) irradiated with either 900 cGy or 400 cGy and performed longitudinal BLI on the irradiated BALB.B hosts. Overall, allogeneic BALB/B recipients showed a dramatic BLI signal increase within the first 8 days after transfer of B6.Luc^{Tg} splenocytes in both cases (Fig. 3A). Soon after transfer, injected donor cells were trapped in the lung and spleen (0 h). The spleen, cervical lymph node, and lymph nodes in the abdominal region were then the major sites emitting distinctively strong BLI signals by day 4 after transfer.

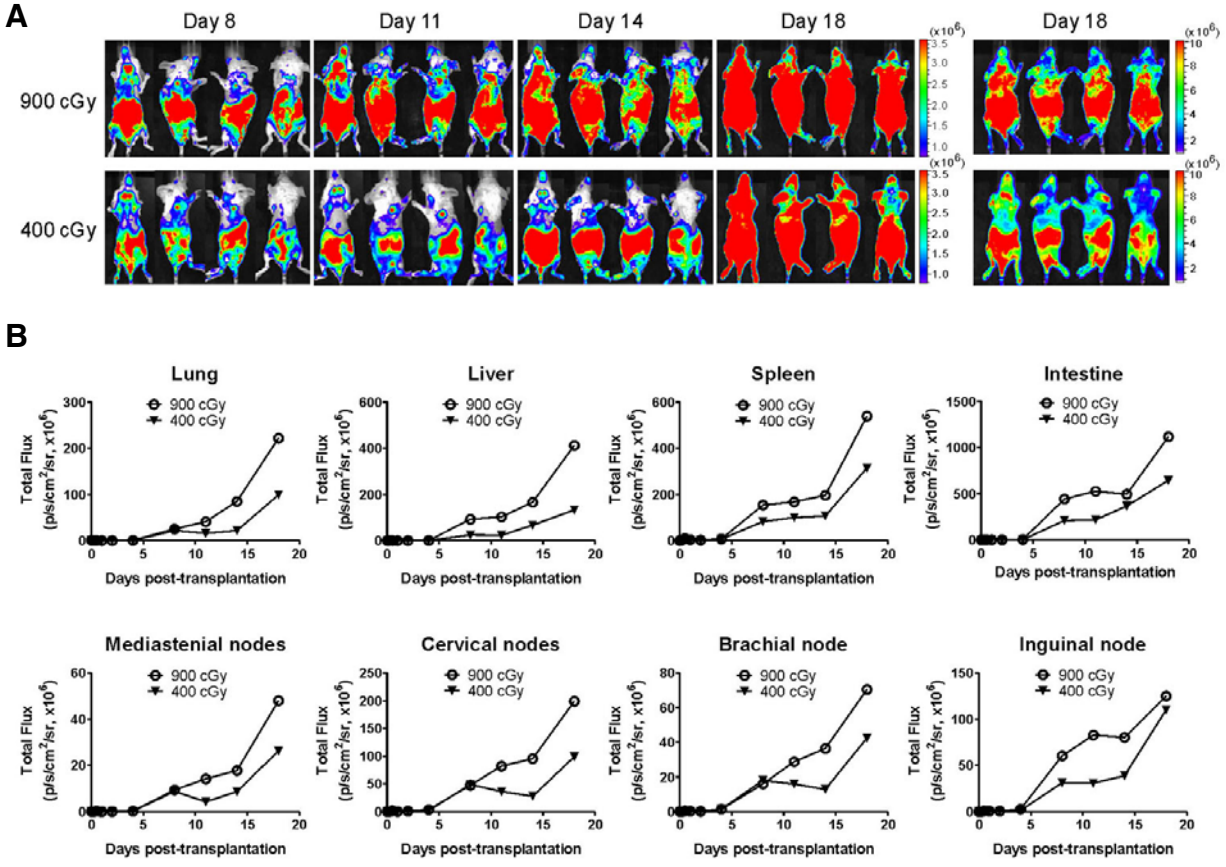

Fig. 4. Long term kinetics of bioluminescence intensity after graft-versus-host disease (GVHD) induction in hosts pre-conditioned with different irradiation doses. (A) The donor cell distribution in the different groups along with GVHD development was monitored. One mouse from each group is shown. (B) The photon outcomes from each region of interest (ROI) were plotted along the time course for long-term events. ROIs were defined for target organs and secondary lymphoid organs. All conditions for irradiation and transplantation were as described in Fig. 3.

The signal spread to the skin by day 8.

Different kinetics of photoemission in target tissues early after transplantation between the GVHD BALB.B hosts irradiated with different doses

To compare the proliferation and migration kinetics of donor cells in GVHD hosts given different irradiation doses, we specifically focused on early BLI signals detected by day 4 post-transplantation in the target organs (lung, intestine, spleen, and liver) by defining the ROIs and measuring the photon flux values corresponding to each ROI (Fig. 3B). The photon output values measured at each time point were then plotted as kinetic curves of total photon flux.

In the BALB.B recipients irradiated with 900 cGy, the spleen showed strong initial signals (5.0×10^5 $s^{-1}cm^{-2}sr^{-1}$ on average) right after transplantation (0 h) with a subsequent signal increase up to 30-fold (1.5×10^7 $s^{-1}cm^{-2}sr^{-1}$ on average) at 12 h post-transplantation, forming an early small peak. After waning in intensity by day 2, it increased again to 23-fold higher (1.1×10^7 $s^{-1}cm^{-2}sr^{-1}$ on average) than the initial value by day 4 post-transplantation. The initial strong signal was also detected in the lung (7.8×10^5 $s^{-1}cm^{-2}sr^{-1}$ on average). The intensity decreased after 5 h, implying migration out of the trapped cells from the lung, and then increased at 12 h post-transplantation, forming an early small peak with an average value of 9.7×10^5 $s^{-1}cm^{-2}sr^{-1}$. The kinetics of photon flux from the intestine and liver were similar to that from the spleen and lung, with early small peaks detected 12 h post-transplantation with average values of 2.3×10^6 $s^{-1}cm^{-2}sr^{-1}$ and 5.7×10^5 $s^{-1}cm^{-2}sr^{-1}$, respectively. The detection of early small peaks in each target organ at 12 h post-transplantation suggested that donor cells would go through a few rounds of cell proliferation in a synchronous manner within the different target organs of 900 cGy-irradiated BALB.B hosts early after transplantation. The average intensities reached by day 4 post-transplantation were 8.8×10^6 $s^{-1}cm^{-2}sr^{-1}$ (23-fold increase of initial value), 1×10^6 $s^{-1}cm^{-2}sr^{-1}$ (5-fold increase), and 7×10^5 $s^{-1}cm^{-2}sr^{-1}$ (0.9-fold increase) for the intestine, liver, and lung, respectively.

For BALB.B hosts irradiated with 400 cGy, the initial signal intensity from the spleen (5.8×10^5 $s^{-1}cm^{-2}sr^{-1}$, on average) was similar to that detected in the 900 cGy group. And the overall kinetics during the first four days in the former was also similar to that observed in the latter, with early small peak detected at 12 h, even though the peak intensity was lower (8.6×10^6 $s^{-1}cm^{-2}sr^{-1}$) than that of the latter. However, in the other target organs (intestine, liver, and lung), the early small peak in BLI signal intensity did not occur at 12 h. Instead, it occurred at 5 h post-transplantation, with lower average peak values of 2.0×10^6 $s^{-1}cm^{-2}sr^{-1}$, 3.2×10^5 $s^{-1}cm^{-2}sr^{-1}$, and 7.5×10^5 $s^{-1}cm^{-2}sr^{-1}$ for the intestine, liver, and lung, respectively, compared to those detected in the 900 cGy. Not only the peak values, but also the intensities reached by day 4 post-transplantation were lower in

the 400 cGy hosts (5.3×10^6 $s^{-1}cm^{-2}sr^{-1}$, 6.6×10^5 $s^{-1}cm^{-2}sr^{-1}$, and 7.1×10^5 $s^{-1}cm^{-2}sr^{-1}$ in the intestine, liver, and lung, respectively). Altogether the data from the BLI study demonstrated that early proliferation within the different target organs was not synchronized in the 400 cGy hosts and the extent of the donor cell expansion was not so high as that in the 900 cGy hosts, illustrating the influence of pre-conditioning dose on the kinetics and degree of early proliferation of donor cells in each target organ.

The de-synchronized early proliferation of donor cells in the target organs of 400 cGy hosts suggested that the early proliferation occurs independently in each target organ after transplantation. Then, we compared the kinetics of BLI intensity from secondary lymphoid organs between the hosts with 900 cGy and 400 cGy, to see if the de-synchronization would be target organ-specific phenomenon or be relevant to secondary lymphoid organs as well. Several different lymph nodes (mediastenial, cervical, brachial, and inguinal lymph nodes) were selected as ROIs for the comparison. Unexpectedly, the early kinetics of photon emission from the lymph nodes was very similar between the GVHD hosts given the two different irradiation doses, with early peaks observed in all lymph nodes at 12 hr post-transplantation. This demonstrates that donor cell kinetics in the secondary lymphoid organs is less dependent on the pre-conditioning dose, indicating significance of irradiation doses on the donor cell kinetics *in situ* at the target organs, rather than in the secondary lymphoid organs. Moreover, it implies that the *in situ* donor cell proliferation occurs immediately after trapping in the target organs, before the tissue infiltration of cells activated in the secondary lymphoid organs.

Similar photon emission kinetics at late time points after transplantation between GVHD BALB.B hosts given different doses of irradiation

The BLI signal spread to the skin by day 8 post-transplantation and continued to increase in all regions by day 18 post-transplantation (Fig. 4A). Overall BLI signal distribution pattern was similar between the hosts with 900 cGy and 400 cGy, but the signal intensities emitted from all the organs of BALB.B hosts irradiated with 900 cGy were higher than those given 400 cGy throughout the observation period. Since BALB.B hosts irradiated with 900 cGy were moribund, we could not continue the BLI beyond day 18 post-transplantation.

When the long-term kinetics of BLI signal intensity was compared between the GVHD hosts irradiated with 900 cGy and 400 cGy (Fig. 4B), all the target organs (spleen, liver, lung, and intestine) and secondary lymphoid organs (mediastenial, cervical, brachial, and inguinal nodes) showed similar kinetic curves in both groups: there was a steady increase in photon emission between days 4 and 14, and a steep increase by day 18. Despite the similarity in kinetic curves between the two groups, the intensity values were quite different. For example, the intestine showed the greatest increase in BLI signal intensity in both groups, but the values reached by day 18 post-transplantation were 11×10^8 $s^{-1}cm^{-2}sr^{-1}$ (4,600-fold as compared with initial values) and 6.4×10^8 $s^{-1}cm^{-2}sr^{-1}$ (1,800-fold) in the 900 cGy and 400 cGy groups, respectively. In addition, the spleen (1,800-fold: 5.4×10^8 $s^{-1}cm^{-2}sr^{-1}$ versus 650-fold: 3.1×10^8 $s^{-1}cm^{-2}sr^{-1}$) and liver (2,000-fold: 4.1×10^8 $s^{-1}cm^{-2}sr^{-1}$ versus 568-fold: 1.3×10^8 $s^{-1}cm^{-2}sr^{-1}$) showed intermediate increase of BLI signal intensity in both groups (900 cGy versus 400 cGy groups, respectively). Lung showed the least increase in the both 900 cGy (260-fold) and 400 cGy (100-fold) groups (2.2×10^8 $s^{-1}cm^{-2}sr^{-1}$ and 1.0×10^8 $s^{-1}cm^{-2}sr^{-1}$, respectively) at the end of the observation period (18 days post-transplantation).

BLI signals intensities from secondary lymphoid organs also increased to a greater extent in the 900 cGy group (600~3,000-fold) as compared with the 400 cGy group (600~2,000-fold). However, in overall, signal intensity emitted from the secondary lymphoid organs were lower than those from the target organs, indicating infiltration of donor cells and further expansion in the target organs at later time points after transplantation.

In summary, overall long-term kinetic curves are considered to be similar between the two groups and consist of three phases: early (between 0 h and 4 days post-transplantation), intermediate (between 4 and 14 days post-transplantation), and late (after 14 days post-transplantation) phases. Over the long term, the kinetic curves of the BLI signal intensities in the 900 cGy and 400 cGy groups diverged around days 4 and 8 (the intermediate phase). And they demonstrate stronger BLI signals in every tissues of 900 cGy than those of 400 cGy, suggesting that this difference in the signal intensities in the long term is a reflection of differences initiated at the target organs *in situ* early after transplantation.

DISCUSSION

In this study, we generated a transgenic mouse line that expresses luciferase in all tissues on a B6 genetic background (B6.luc^{Tg}) and obtained BLI results after GVHD induction using the B6.luc^{Tg} mice as the donor strain for BM and splenocytes. Possessing transgenic mice with efficient luciferase enzyme activity and normal immunological characteristics on a B6 genetic background (B6.Luc^{Tg}) enabled us to investigate donor cell dynamics in MHC-matched allogeneic GVHD hosts and the effects of irradiation on those dynamics.

We monitored donor cell proliferation and migration in MHC-matched allogeneic GVHD hosts after transplantation of BM and splenocytes from B6.Luc^{Tg} mice. In terms of donor cell migration and proliferation, our data show that transplanted donor cells are first trapped in the lung and spleen, which is consistent with results from other studies (Beilhack et al., 2005; Ushiki et al., 2010). Secondary lymphoid organs, such as the mesenteric lymph node, spleen, and Peyer's patches, have been thought to be the initial sites of acute GVHD, in which donor T cells are activated and proliferate (Murai et al., 2003; Panoskaltsis-Mortari et al., 2004). In MHC-mismatched GVHD hosts, homing of donor T cells was detected in the T cell zones of the lymph nodes within 12 h post-transplantation (Beilhack et al., 2005). They were found to be confined to the lymph node by day 3 before infiltration into target tissues. Splenectomy and prevention of T cell entry into all secondary lymphoid organs with anti-CD62L monoclonal antibody abrogated the onset of gut GVHD, supporting the importance of T cell activation in the secondary lymphoid organs (Beilhack et al., 2008). Our data also showed donor cell expansion in the secondary lymphoid organs and donor cell spread to the skin in MHC-matched allogeneic GVHD hosts, similar to that previously reported using MHC-mismatched GVHD systems (Negrin and Contag, 2006).

Additionally, comparison of donor cell dynamics between hosts given two different irradiation doses revealed that early donor cell proliferation in the target organs is as important as in the secondary lymphoid organs. Donor cell proliferation in the target organs and secondary lymphoid organs seems to occur in a synchronized fashion early after GVHD induction in hosts irradiated with 900 cGy, but not 400 cGy, demonstrating the influence of pre-conditioning doses on the *in vivo* dynamics of donor cells. The photon flux intensities from the target organs at the early peak times are also higher in the former than the latter, implying different degrees of early proliferation of donor cells in

the target organs of GVHD hosts given different doses of irradiation. Based on these results, we suggest that donor cells trapped in the liver, lung, and spleen, in addition to those in the secondary lymphoid organs, also go through a few rounds of proliferation *in situ* early after transplantation, prior to infiltration into the target organs. The irradiation effect appears very early after transplantation. At this time, we are not aware of exactly what cell types go through early *in situ* proliferation, since we did not perform a subtyping analysis on the donor cells in this study. It is possible that macrophages and granulocytes are activated by irradiation-induced inflammation or T cells may be activated by recognition of allo-antigens presented by regional antigen presenting cells, such as myeloid and plasmacytoid dendritic cells (DC) in the liver (Shlomchik et al., 1999; Thomson and Knolle, 2010; Zhang et al., 2002). Whatever the subtype of cells that go through *in situ* proliferation, the degree of *in situ* early proliferation is closely related to the further expansion of donor cells after infiltration into the target organs and with the severity of GVHD. We assume that in hosts irradiated with 400 cGy, the early proliferation of donor cells trapped in the same places is limited, because of less severe tissue damage by the lower dose of irradiation or killing of the donor cells by the host immune cells that survive irradiation. This results in the formation of only very small early peaks of total flux at 5 h post-transplantation.

Despite its significance as a risk factor for GVHD (Ferrara et al., 2009), the influence of pre-conditioning doses on the dynamics of donor cells *in vivo*, especially under MHC-matched allogeneic conditions, has never been evaluated. The results from this study show different kinetics and degrees of proliferation *in situ* early after transplantation in the target organs of GVHD hosts, depending on the pre-conditioning irradiation doses. To our knowledge, we are the first to monitor donor cell dynamics in GVHD hosts after MHC-matched allogeneic transplantation and to investigate the effects of pre-conditioning on the dynamics *in vivo*. We consider that these results will provide helpful information on the pathophysiology of GVHD and aid in the development of preventative measures for GVHD.

ACKNOWLEDGMENTS

The codon optimized luciferase was kindly provided by Dr. Brian A. Ravinovich from MD Anderson Cancer Center, University of Texas, Houston, TX. This study was supported by a grant from the Korean Health Technology R&D Project, Ministry for Health, Welfare & Family Affairs, Republic of Korea (A084308). There is no conflict of interest among the authors regarding this manuscript.

REFERENCES

Beilhack, A., Schulz, S., Baker, J., Beilhack, G.F., Wieland, C.B., Herman, E.I., Baker, E.M., Cao, Y.A., Contag, C.H., and Negrin, R.S. (2005). *In vivo* analyses of early events in acute graft-versus-host disease reveal sequential infiltration of T-cell subsets. Blood *106*, 1113-1122.

Beilhack, A., Schulz, S., Baker, J., Beilhack, G.F., Nishimura, R., Baker, E.M., Landan, G., Herman, E.I., Butcher, E.C., Contag, C.H., et al. (2008). Prevention of acute graft-versus-host disease by blocking T-cell entry to secondary lymphoid organs. Blood *111*, 2919-2928.

Cao, Y.A., Bachmann, M.H., Beilhack, A., Yang, Y., Tanaka, M., Swijnenburg, R.J., Reeves, R., Taylor-Edwards, C., Schulz, S., Doyle, T.C., et al. (2005). Molecular imaging using labeled donor tissues reveals patterns of engraftment, rejection, and survival in transplantation. Transplantation *80,* 134-139.

Choi, E.Y., Yoshimura, Y., Christianson, G.J., Sproule, T.J., Malarkannan, S., Shastri, N., Joyce, S., and Roopenian, D.C. (2001). Quantitative analysis of the immune response to mouse non-MHC transplantation antigens *in vivo*: the H60 histocompatibility antigen dominates over all others. J. Immunol. *166*, 4370-4379.

Choi, E.Y., Christianson, G.J., Yoshimura, Y., Jung, N., Sproule, T.J., Malarkannan, S., Joyce, S., and Roopenian, D.C. (2002a). Real-time T-cell profiling identifies H60 as a major minor histocompatibility antigen in murine graft-versus-host disease. Blood *100*, 4259-4265.

Choi, E.Y., Christianson, G.J., Yoshimura, Y., Sproule, T.J., Jung, N., Joyce, S., and Roopenian, D.C. (2002b). Immunodominance of H60 is caused by an abnormally high precursor T cell pool directed against its unique minor histocompatibility antigen peptide. Immunity *17*, 593-603.

Choi, J.H., Yoon, H., Min, C.K., and Choi, E.Y. (2011). Effects of pre-conditioning dose on the immune kinetics and cytokine production in the leukocytes infiltrating GVHD tissues after MHC-matched transplantation. Immun. Netw. *11*, 68-78.

Ferrara, J.L., Levy, R., and Chao, N.J. (1999). Pathophysiologic mechanisms of acute graft-vs.-host disease. Biol. Blood Marrow Transplant *5*, 347-356.

Ferrara, J.L., Levine, J.E., Reddy, P., and Holler, E. (2009). Graft-versus-host disease. Lancet *373*, 1550-1561.

Korngold, R., and Wettstein, P.J. (1990). Immunodominance in the graft-vs-host disease T cell response to minor histocompatibility antigens. J. Immunol. *145*, 4079-4088.

Murai, M., Yoneyama, H., Ezaki, T., Suematsu, M., Terashima, Y., Harada, A., Hamada, H., Asakura, H., Ishikawa, H., and Matsushima, K. (2003). Peyer's patch is the essential site in initiating murine acute and lethal graft-versus-host reaction. Nat. Immunol. *4*, 154-160.

Negrin, R.S., and Contag, C.H. (2006). *In vivo* imaging using bioluminescence: a tool for probing graft-versus-host disease. Nat. Rev. Immunol. *6*, 484-490.

Panoskaltsis-Mortari, A., Price, A., Hermanson, J.R., Taras, E., Lees, C., Serody, J.S., and Blazar, B.R. (2004). *In vivo* imaging of graft-versus-host-disease in mice. Blood *103*, 3590-3598.

Rabinovich, B.A., Ye, Y., Etto, T., Chen, J.Q., Levitsky, H.I., Overwijk, W.W., Cooper, L.J., Gelovani, J., and Hwu, P. (2008). Visualizing fewer than 10 mouse T cells with an enhanced firefly luciferase in immunocompetent mouse models of cancer. Proc. Natl. Acad. Sci. USA *105*, 14342-14346.

Roopenian, D., Choi, E.Y., and Brown, A. (2002). The immunogenomics of minor histocompatibility antigens. Immunol. Rev. *190*, 86-94.

Shlomchik, W.D. (2007). Graft-versus-host disease. Nat. Rev. Immunol. *7*, 340-352.

Shlomchik, W.D., Couzens, M.S., Tang, C.B., McNiff, J., Robert, M.E., Liu, J., Shlomchik, M.J., and Emerson, S.G. (1999). Prevention of graft versus host disease by inactivation of host antigen-presenting cells. Science *285*, 412-415.

Thomson, A.W., and Knolle, P.A. (2010). Antigen-presenting cell function in the tolerogenic liver environment. Nat. Rev. Immunol. *10*, 753-766.

Ushiki, T., Kizaka-Kondoh, S., Ashihara, E., Tanaka, S., Masuko, M., Hirai, H., Kimura, S., Aizawa, Y., Maekawa, T., and Hiraoka, M. (2010). Noninvasive tracking of donor cell homing by near-infrared fluorescence imaging shortly after bone marrow transplantation. PLoS One *5*, e11114.

Weissleder, R., and Pittet, M.J. (2008). Imaging in the era of molecular oncology. Nature *452*, 580-589.

Yoon, S.R., Chung, J.W., and Choi, I. (2007). Development of natural killer cells from hematopoietic stem cells. Mol. Cells *31*, 1-8.

Zhang, Y., Shlomchik, W.D., Joe, G., Louboutin, J.P., Zhu, J., Rivera, A., Giannola, D., and Emerson, S.G. (2002). APCs in the liver and spleen recruit activated allogeneic CD8+ T cells to elicit hepatic graft-versus-host disease. J. Immunol. *169*, 7111-7118.